NASA TN D-1096

TECHNICAL NOTE

D-1096

INFRARED AND REFLECTED SOLAR RADIATION MEASUREMENTS FROM THE TIROS II METEOROLOGICAL SATELLITE

W. R. Bandeen, R. A. Hanel,
John Licht, R. A. Stampfl, and W. G. Stroud

Goddard Space Flight Center
Greenbelt, Maryland

NATIONAL AERONAUTICS AND SPACE ADMINISTRATION
WASHINGTON

November 1961

INFRARED AND REFLECTED SOLAR RADIATION MEASUREMENTS FROM THE TIROS II METEOROLOGICAL SATELLITE

by

W. R. Bandeen, R. A. Hanel,
John Licht, R. A. Stampfl, and W. G. Stroud
Goddard Space Flight Center

SUMMARY

TIROS II contains instrumentation for measuring infrared and reflected solar radiation from the earth and its atmosphere. A medium resolution scanning radiometer and a low resolution non-scanning radiometer are employed. The satellite's spin provides the scan line of the medium resolution radiometer which is then advanced by the orbital motion. The spatial resolution is about 40 miles square when the earth directly beneath the satellite is viewed. The five channels employ bolometer detectors and filters to limit the spectral responses to five bands: 6 to 6.5 μ, 8 to 12 μ, 0.2 to 6 μ, 8 to 30 μ, and 0.55 to 0.75 μ. These five bands study, respectively: radiation in the water vapor absorption band; day and nighttime cloud cover; albedo; thermal radiation; and visual maps for comparison with satellite vidicon pictures. The low resolution non-scanning radiometer measures the earth's black-body temperature and albedo. Its field when viewing directly below is a circle of 450 miles diameter, covering part of each frame from the wide-field television camera. This radiometer consists of two thermistors, each in the apex of a reflective cone which provides optical gain. One thermistor is black and responds to both thermal and reflected solar radiation. The second responds to thermal but reflects solar radiation. The design, calibration, performance, and data reduction for both systems are discussed herein.

CONTENTS

D-1096

INFRARED AND REFLECTED SOLAR RADIATION MEASUREMENTS FROM THE TIROS II METEOROLOGICAL SATELLITE

by

W. R. Bandeen, R. A. Hanel,
John Licht,* R. A. Stampfl, and W. G. Stroud
Goddard Space Flight Center

INTRODUCTION

The TIROS II (1960 π_1) meteorological satellite (Figure 1) was launched on November 23, 1960. Its orbital characteristics are compared to those of TIROS I (1960 β) in Table 1. Like its predecessor, TIROS II carries two television cameras. Although pictures from the wide angle camera are not equivalent to their TIROS I counterparts in quality, the TIROS II television system has worked with considerable success. The functioning of the television system, which is practically equivalent to that of TIROS I, has been reported (References 1 and 2) and will not be discussed here.

Table 1
Orbital Characteristics of TIROS I and TIROS II

Orbital Characteristics	TIROS I (Launched April 1, 1960)	TIROS II (Launched November 23, 1960)
Perigee (statute miles)	432.9	385.6
Apogee (statute miles)	464.4	454.4
Period (minutes)	99.24	98.27
Inclination (degrees)	48.39	48.53

*Now with Lockheed Electronics Corporation

The outstanding difference between the two satellites was the inclusion in TIROS II of an experiment consisting of two radiometers to measure the infrared and reflected solar radiation from the earth and its atmosphere.

DESCRIPTION OF THE EXPERIMENT

The TIROS II radiation experiment consists of: a medium resolution five-channel scanning radiometer with its bi-directional optical axes inclined to the spin axis by angles of 45 and 135 degrees; and a low resolution two-channel non-scanning radiometer whose optical axes are parallel to the spin axis. As the satellite spins, the 5-degree field of view of each medium resolution radiometer channel scans alternately the earth and outer space. The orbital motion provides the advancement from one sweep line to the next. A spin rate of about 12 rpm was chosen to accommodate a proper scan pattern, a raster without overlap or underlap of individual lines. The spin rate is consistent with the available information bandwidth of 8 cps per channel. A scan line is given by the intersection of the 45-degree half-angle cone described by the optical axis of the detectors in one spin cycle, and the earth's nearly spherical surface. When the spin axis is parallel to the local earth radius vector, the scan pattern is a circle on the earth; it becomes a pair of alternating, hyperbola-like branches wherever the spin vector is normal to the radius vector. The geometry of the motion is identical to the geometry which the Vanguard II cloud cover satellite was intended to (but actually did not) assume (Reference 3). The satellite spin, however, does not modulate the 50-degree field-of-view low resolution radiometer channels because their optical axes are parallel to the spin axis. The low resolution radiometer observes an area which is within the field of the wide angle TV camera; thus interesting correlations between cloud cover and heat balance may be expected. Figure 2 illustrates the geometry of the scanning motion of the medium resolution radiometer and that of the viewing area of the low resolution radiometer.

The instrument in the satellite measures radiation intensities in a certain direction and from a certain area, the area in the field of view. If the scattering function of this area were known, the total amount of back-scattered energy, the albedo, could be computed. However, the area in the field of view neither reflects nor radiates according to Lambert's law like a perfectly diffuse surface; therefore assumptions must be made about the non-isotropic nature of radiation in order to arrive at the total radiation loss in all directions (Reference 4). Calculations on the non-isotropic nature of radiation emerging from the atmosphere can be based on model atmospheres. The satellite observes certain areas on the earth's surface under different zenith angles within a time interval as short as three minutes. Results of these observations will tend to verify the choice of a particular model atmosphere in a given region (References 5 and 6).

In the medium resolution radiometer, lens materials and filters restrict the sensitivities of the five channels to the following spectral regions:

(1) 6 to 6.5 microns—water vapor absorption;
(2) 8 to 12 microns—atmospheric window;
(3) 0.2 to 6 microns—reflected solar radiation;
(4) 8 to 30 microns—thermal radiation;
(5) 0.55 to 0.75 microns—visible reference and daytime cloud cover.

The physical significance of these regions has been reported previously (Reference 7) and will be discussed only briefly here.

In Figure 3 the transmission characteristic of the filters of channels 3 and 5 are plotted against the available energy from a blackbody at 5800°K, the color temperature of the sun. About 99 percent of back-scattered and reflected sunlight falls into the spectral range of channel 3. The spectral range of channel 5 was chosen to give good contrast between earth and clouds; it is in the range of visible and infrared photography and close to the spectral sensitivity of the TIROS television cameras. This channel yields cloud cover pictures on the illuminated side of the earth, while the television system covers only limited areas, although with much higher resolution.

Figure 4 shows the transmission characteristics of the three thermal channels (1, 2, and 4). The abscissa is linearly proportional to the energy available from a 300°K blackbody. Neither the emissivity of the thermistor bolometer nor the chopper characteristic is included in the diagram. The spectrum of channel 4 (8 to 30 microns) covers fairly well the range of thermal emission from the earth. In a study of the energy budget, the total amount of radiation loss is even more important than the albedo. Channel 2 measures radiation emerging in the atmospheric "window" between 8 and 12 microns. Since the atmosphere is fairly transparent in this spectral range, the apparent blackbody temperatures are close to the true temperatures of the radiation surfaces, whether they be cloud tops, water, or land. Corrections must be made for ozone absorption near 9.6 microns. Because clouds are generally cooler than the earth's surface, a map showing isolines of radiant emittance can be interpreted as a cloud cover map. This method is especially valuable since it also works on the dark side of the earth, which is unobserved by television cameras. The difference between the channel 4 and the channel 2 measurements is essentially the radiation between 12 and 30 microns, characterized by strong absorption bands of carbon dioxide and water vapor. Channel 1 responds to radiation in the region of water vapor absorption, between 6 and 6.5 microns. The temperature profile and relative humidity of the atmosphere determine the energy which can be observed by this channel.

The spin vector of TIROS I exhibited angular motions of large amplitude during its 78-day active life. These compared closely with a theoretical model based upon reactions

to two external torques, namely: a primary torque caused by the interaction of a magnetic dipole along the satellite spin axis with the earth's magnetic field; and a secondary torque caused by differential gravity in the earth's field (Reference 8). Because of the importance of keeping the radiation sensors from viewing the sun for any longer than was absolutely necessary, TIROS II contains a closed current loop with several possible levels of current flow, both positive and negative, any one of which can be commanded from the ground. Thus the motion of the satellite spin axis can in some measure be controlled. This magnetic Attitude Control works satisfactorily and the observed spin axis motions, after specific current values were programmed in the coil, agreed well with calculated theoretical movements.

Spin-up rockets attached to the periphery of the satellite's base plate can be fired by ground command, either to achieve the desired spin rate if the de-spin after injection results in too low a rate, or to restore the desired level after magnetic spin-decaying effects have operated for a time. Two pairs of spin-up rockets were fired two days after the launching, increasing the spin rate from 8.0 rpm to 14.0 rpm.

INSTRUMENTATION

One channel of the medium resolution radiometer is depicted in Figure 5. The chopper disk, which is half reflecting and half absorbing, reflects radiation alternately from the scan beam and the reference beam to the detector. Consequently, the alternating voltage generated at the thermistor bolometer is proportional to the energy difference between the two opposite directions. The radiometer is shown in Figure 6.

The two low resolution radiometer channels consist of a black and a white detector, each mounted in the apex of a highly reflective cone (Figure 7 and Reference 9). The black detector is equally sensitive to reflected sunlight and long-wavelength terrestrial radiation. The white detector is coated to be reflective in the visible and near infrared; its surface appears white to the eye even though its emissivity is high in the far infrared. Since 99.9 percent of the terrestrial radiation is emitted at wavelengths of 4 microns and longer, both detectors have the same equilibrium temperature when they face the dark side of the earth. On the illuminated side of the earth the temperature of the black detector rises in contrast to that of the white, which is affected to a lesser extent by reflected sunlight. Careful measurements of the temperatures of the detectors and the mounting plate, as well as a determination of thermal conduction and radiation coupling between thermistor flake and satellite, permits the determination of the apparent blackbody temperature and the amount of reflected sunlight within the 50-degree field of view of the instrument.

Before installation in the satellite, the radiometers had to pass a series of environmental tests and calibration measurements. In order to calibrate its three thermal channels, the medium resolution radiometer was exposed to two blackbodies. One, simulating outer space, had the temperature of liquid nitrogen. The second blackbody, which simulated radiation from the earth, was adjusted to various temperatures between 250° and 320°K. To minimize errors from water vapor absorption and to prevent condensation on the cold targets, the radiometer and the blackbodies were placed in a dry nitrogen atmosphere. The response V of a channel is proportional to the energy difference between opposite directions, expressed by

$$V = k \int_0^\infty [W_\lambda(T_1) - W_\lambda(T_2)] f_\lambda \, d\lambda . \qquad (1)$$

where $W_\lambda(T_1)$ and $W_\lambda(T_2)$ are the spectral radiant emittances of the blackbodies, and f_λ is the filter function for the channel in question. The emissivity of the bolometer and reflectivity of the chopper are considered independent of wavelength. This is fairly well justified for all but the 8 to 30 micron channel. The second part of the integral in Equation 1 is negligible for liquid nitrogen temperatures but has to be taken into account if T_1 and T_2 are at room temperature or slightly above. The latter temperatures existed in a check of calibration at Cape Canaveral where the whole system, including radiometer and telemetering electronics, was tested. The constant k includes also the gain of the preamplifier. In the calibration the gain was set to give the same maximum voltage in each channel for different blackbody temperatures: 265°, 315°, and 305°K for channels 1, 2, and 4 respectively.

The standard source in the calibration of the two solar channels of the medium resolution radiometer (0.2 to 6 and 0.55 to 0.75 microns) was a tungsten band lamp with a quartz window. It was necessary to make extensive corrections because of the difference between the lower color temperature of 2200°K and sun temperatures of about 5800°K. Since the standard lamp is too small to fill the field of view of the radiometer, and its intensity too great, a larger source was used as an intermediate step. The opal glass used in the intermediate step is not quite as diffuse at 2 microns as it is in the visible. Unfortunately this effect was not recognized immediately, and the gain on these two channels was set about 10 decibels too low. However, since the signal-to-noise ratio is good such an error can be compensated for by readjusting the gain in the ground station.

The low resolution radiometer was calibrated in vacuum. It was mounted on a metal frame which simulated the satellite, and the temperature of the frame was adjusted in steps between -10° and +60°C. Radiation from the earth was simulated by a blackbody, which filled the field of view, whose temperature was varied between -130° and +60°C. In this way, heat conduction and radiation coupling between thermistor flakes and satellite

structure were determined. Then the detector, still in vacuum, was exposed to sunlight (and artificial light) reflected by a white diffuser. The transmission characteristic of the quartz window which sealed the vacuum chamber was taken into account. A thermopile served as the calibration standard.

The radiation experiment instrumentation is independent of the television camera system except for power, command, certain timing signals, and antennas (Figures 8 and 9). The outputs of the five narrow angle radiometer channels are fed to five subcarrier oscillators. These voltage controlled oscillators are of the phase shift type, with symmetric amplifiers in the feedback loops, the gains of which are controlled by the balanced input signal.

A sixth channel telemeters the wide-angle low-resolution sensor data, environmental temperatures, instrumentation canister pressure, and calibration. A mechanical commutator switches resistive sensors in one branch of a phase shift oscillator. The seventh channel, a tuning fork oscillator, serves as a reference frequency and timing signal. The outputs from these seven different channels are added and the resultant composite signal is equalized in a record amplifier which drives the head of a miniature tape recorder.

An oscillator provides an alternating current bias to the record head and also provides the signal required for the erase head. For convenience, erasure of the magnetic tape occurs immediately before recording. The record spectrum extends from 100 to 550 cps. The tape recorder is an endless loop two-speed design, running at 0.4 in./sec record speed and 12 in./sec playback speed. The endless loop records continuously except during a playback sequence. A hysteresis synchronous motor generates torque in the record mode through a mylar belt speed reduction system (Reference 10). The fourth subharmonic of the tuning fork oscillator, generated by flip flops, drives the motor. The record motor also drives a cam shaft which activates a bank of micro switches connected to the five commutated sub-channels of the time-sharing sixth channel. Each is sampled every six seconds, and the fifth includes a group of seven to be sub-commutated.

Playback begins upon command, by applying power to a direct current motor. A magnetized flywheel generates a frequency proportional to the motor speed. A frequency discriminator feeds the error signal to the stabilized power supply of the motor and closes the servo loop. Playback speed is essentially constant from 0° to 50°C. A low flutter and wow, 2.5 percent peak to peak measured without frequency limitations, is achieved by using precision bearings and ground-in-place shafts with tolerances better than 50 parts per million. A command pulse activates the playback motor, the playback amplifier, and the 238-Mc FM telemetry transmitter feeding the duplexer and antenna.

To permit comparison of the low resolution measurements with TV pictures, each TV shutter action generates a 1.5 second pulse which is recorded as an amplitude

modulation of the channel 7 timing signal. As in TIROS I, there are nine solar cells mounted behind narrow slits for north angle determination. These slits have an opening angle of close to 180 degrees in planes through the spin axis. The sun illumination generates pulses as long as there is no illumination parallel to the spin axis. One of these sensors generates a 0.5 second pulse in addition to the north indicator code, so that spin rate information and a measure of relative sun position is available. Again, this pulse is recorded as an amplitude modulation of channel 7. Reconstruction of the radiation information vitally depends on its correlation with absolute time. The tuning fork oscillator provides an accurate but relative timing signal; and the sun pulses give a crude one, except in the earth's umbra. Absolute time is transmitted to the satellite and recorded on the tape as a 1 second drop-out of channel 7. The occurrence of this pulse is known within milliseconds of absolute time.

OPERATION OF THE EXPERIMENT

Upon interrogation, the 238 Mc carrier from the satellite is received by a 60-foot parabolic antenna; the composite signal is recorded on magnetic tape and, simultaneously, fed to a "Quick-Look" demodulator (Figure 10a). At the same time, the envelope of channel 7 and the clipped signal of channel 4 are graphically recorded. The 8 to 30 micron "events" on the graphic record show the earth and sky scan intervals alternately, and the channel 7 envelope shows the three distinctive types of AM pulses impressed on the clock frequency during the record mode. These pulses are the sun sensor pulses, the TV camera pulses, and the "end-of-tape" pulse. Auxiliary uses of the radiation data include determination of the spin axis attitude in space and the times when television pictures were taken and recorded in the satellite, to be read out later over a ground station (Figure 10b).

Every day the magnetic tapes are mailed to the Aeronomy and Meteorology Division, Goddard Space Flight Center, Greenbelt, Maryland. The master tape containing the composite radiation signal is demultiplexed, demodulated, and fed to an analog-to-digital converter (Figure 11). The pressure is read separately. The analog-to-digital converter produces a magnetic "Radiation Data Tape" of 36-bit words suitable for an IBM 7090 computer. In addition to the digital magnetic tape for routine analyses on a computer, an analog record may be produced on an oscillograph for special hand analyses. The initial reduction of data from orbit "0", discussed later in this paper, was carried out in this way.

The IBM 7090 computer program of the U. S. Weather Bureau's Meteorological Satellite Laboratory requires inputs from three sources to produce the "Final Meteorological Radiation Tape" (Figure 12). One source is the Radiation Data Tape containing radiation and satellite environmental parameters in digital form. A second source is the

"Orbital Tape" from the NASA Space Computing Center, containing satellite position and attitude data. The third is the calibration for converting the digital information to meaningful physical units. The Final Meteorological Radiation Tape, then, is the basic repository of data from the medium resolution scanning radiometer. In order to study and utilize the scanning radiometer data, appropriate computer programs must be written to "talk" to the Final Meteorological Radiation Tape and provide for printing out data, punching cards, or producing maps. It is planned that The National Weather Records Center (NWRC), Asheville, North Carolina, will make copies of the Final Meteorological Radiation Tape available to universities and other interested research groups. A special document will be prepared describing the contents of the Final Meteorological Radiation Tape in technical computer language for users who wish to write their own programs.

Because it is sampled only when TV pictures are taken, the output rate of the non-scanning, low resolution radiometer is vastly smaller than that of the medium resolution radiometer. Hence the non-scanning data will be punched on cards or printed.

PRELIMINARY RESULTS

Samples of data have been reduced by hand analyses to check the computer program and to demonstrate the validity and usefulness of the information. Figure 13 shows three consecutive sweeps of channel 2, recorded on the first pass between Australia and New Zealand. These are typical scan patterns. The base line corresponds to zero radiation level; at that instant both sides of the detector faced outer space. The amplitude is proportional to the energy available within the spectral range of the channel. Detectors, preamplifiers, and voltage controlled oscillators contribute, in the form of non-linearities and temperature dependence, to the final conversion factor between the recorded frequency deviation and the radiation level seen by the detector. Figure 14 shows all channels on a more compressed scale. The amplitude modulation on channel 7 shows sun pulses. The first five patterns are the five channels of the medium resolution radiometer. The commutated channel 6 contains temperatures of the black and white cone and all the "housekeeping" information. The point of verticality, where one detector sweeps a circle on the earth, can be recognized on the right where the horizon is not intercepted at all. Figure 15 shows only the last two channels. The wider pulses on channel 7 are camera shutter signals recorded as pictures were taken every 30 seconds. In Figure 16 the transition between the illuminated and shadowed part of an orbit can be identified by the cessation of sun pulses.

For the analysis, samples were selected from the first orbits over the United States and over the Tasmanian Sea. Conversion factors between frequency deviation and apparent blackbody temperatures were deduced from calibration data. Figure 17 is a plot of the 8 to 12 micron radiation temperatures. Only the point where the optical axis intercepts

the satellite path and two points 10 degrees on either side are shown for sweeps one minute apart. These are less than 1 percent of the available data points. Blackbody temperatures over the Northwestern States varied from 210° to 250°K. The maximum temperatures, recorded in the vicinity of Ohio and of California is close to 280°K. But temperatures over the Eastern States are again lower than this.

A cloud analysis and frontal position map is shown in Figure 18. Areas of low radiation temperatures seem to coincide with the cloud shield very well. The 6 to 6.5 micron map (Figure 19) shows less variation between cloudy and clear areas. Radiation temperatures range from 220°K, over clouds, to 250°K, over cloudless areas. The absolute scale for blackbody temperatures measured by the 8 to 30 micron channel has not yet been established with the same confidence that exists in regard to the other channels. However, the same general pattern can be recognized and results from this channel are expected to fall between those of channels 1 and 2. The relative accuracy of channels 1 and 2 is about ±2°C, although absolute values may shift up and down as much as 5°C as second order effects in the calibration procedure are taken into account.

An area between Australia and New Zealand was reduced to the fullest extent. Figure 20 shows the TIROS radiation map of apparent blackbody temperatures near local midnight. Low temperatures east of the islands indicate clouds probably higher than 5 kilometers. The maximum temperatures registered come close to the surface temperatures of water in this area.

Data from the low resolution radiometer are in Figure 21 together with a nephanalysis for the first four orbits. The temperature of the black thermistor varies considerably between 306°K over Africa and 286°K over the Atlantic Ocean. The temperature of the white thermistor follows the same pattern. A maximum of about 8°C difference in sensor temperatures ($T_B - T_W$) existed over the largely overcast frontal area just south of Greece, but the two temperatures are the same over clear ocean areas where the albedo is low. The temperature difference is smaller than was expected from the calibration data. The white detector seems to act like a "medium gray" sensor; but before final conclusions can be drawn, much more data will have to be analyzed. In spite of lower temperature differences than were expected, the cloud cover analysis is in good agreement with the radiometer data.

CONCLUSION

The radiation experiment of TIROS II, a rather complex electronic and mechanical system, has worked very well. The instruments have produced and are continuing to produce valuable data. The enormous amount of data should be made available to the meteorological community as soon as there is full confidence in all scales which go with

the data, and as soon as the automatic data processing techniques are working entirely satisfactorily.

ACKNOWLEDGMENTS

It is impossible to acknowledge individually the contributions of all the persons who made this program a success. The authors wish to thank the Barnes Engineering Company for the radiometers, the RCA Astro-Electronics Division for the television system and assembly of the satellite, the USWB Meteorological Satellite Laboratory for its effort in the area of data reduction, and the personnel of the Goddard Space Flight Center who designed and built the major part of the radiation experiment instrumentation, performed the calibration, and reduced the data shown. In addition thanks are due to the Optical Branch of the Naval Research Laboratory for participating in the calibration, and to the two Command and Data Acquisition Stations at Point Mugu, California, and Fort Monmouth, New Jersey, for acquiring the data.

REFERENCES

1. Stroud, W. G., "Initial Results of the Tiros I Meteorological Satellite," J. Geophys. Res. 65(5):1643-1644, May 1960
2. Sternberg, S., and Stroud, W. G., "Tiros I: Meteorological Satellite," Astronautics 5(6):32-34 and 84-86, June 1960
3. Hanel, R. A., Licht, J., Nordberg, W., Stampfl, R. A., and Stroud, W. G., "The Satellite Vanguard II: Cloud Cover Experiment," IRE Trans. on Mil. Electronics MIL-4(2 and 3):245-247, April-July 1960
4. Wark, D. Q., and Yamamoto, G., "Methods of Transforming Terrestrial Infrared Radiation Measurements Made from Satellites," paper presented at the 41st Annual Meeting of the AMS, New York, January 23-26, 1961, to be published
5. Greenfield, S. M., and Kellogg, W. W., "Calculations of Atmospheric Infrared Radiation as Seen from a Meteorological Satellite," J. of Meteorol. 17(3):283-290, June 1960
6. Wexler, R., "Satellite Observations of Infrared Radiation," First Semi-Annual Technical Summary Report (Allied Research Associates, Boston, Massachusetts), Contract Number AF19(604) - 5968, ARCRC, December 24, 1959
7. Hanel, R. A., and Stroud, W. G., "Infrared Imaging from Satellites," J. of the SMPTE 69(1):25-26, January 1960

8. Bandeen, W. R., and Manger, W. P., "Angular Motion of the Tiros I Meteorological Satellite Due to Magnetic and Gravitational Torques," J. Geophys. Res. 65(9):2992-2995, September 1960

9. Hanel, R. A., "Low Resolution Unchopped Radiometer for Satellites," ARS J. 31(2):246-250, February 1961; also NASA Technical Note D-485, February 1961

10. Licht, J. H., and White, A., "Polyester-Film Belts," Mach. Des. 32(22):137-143, October 27, 1960; also NASA Technical Note D-668, May 1961

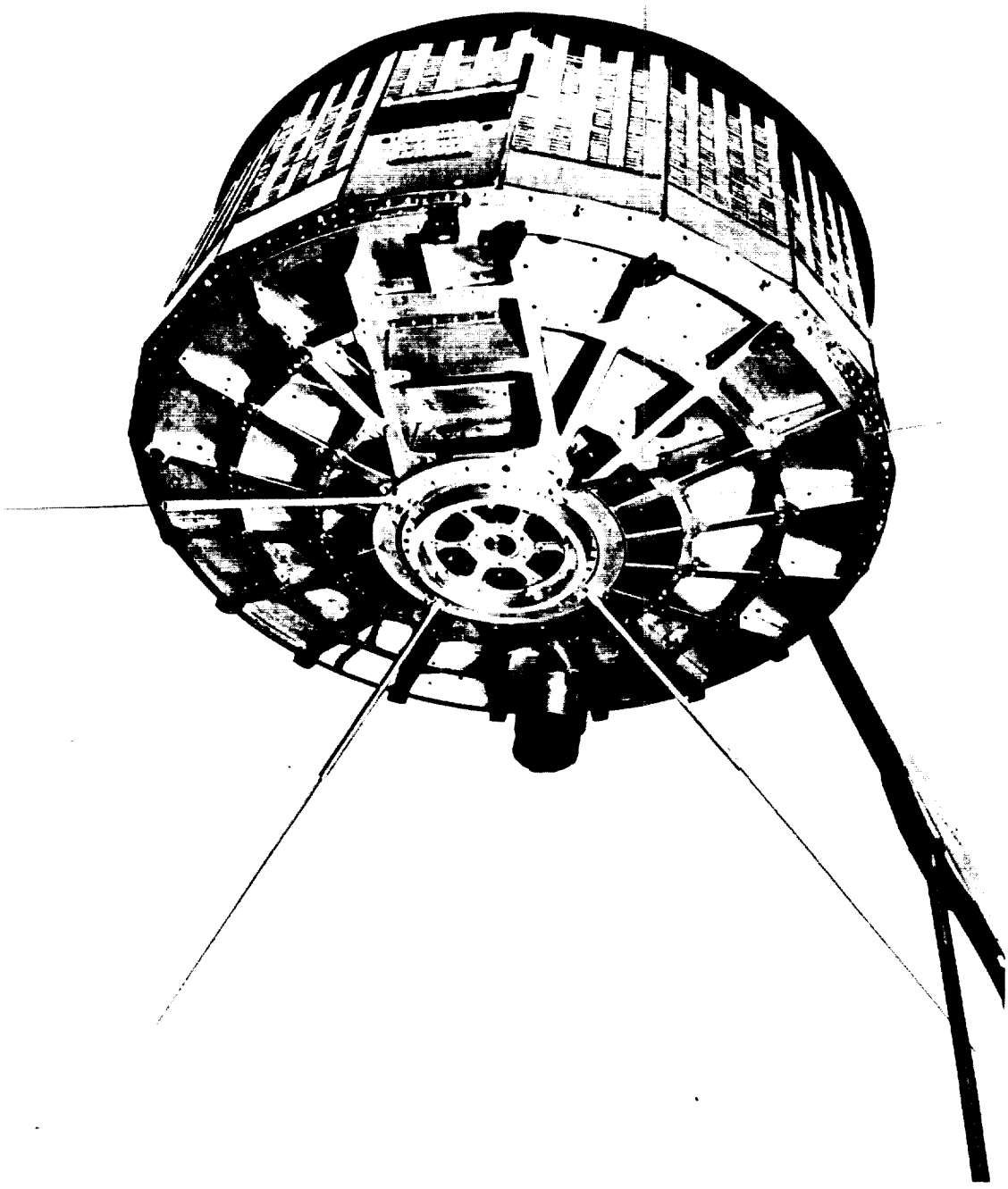

Figure 1—The TIROS II meteorological satellite. The medium resolution scanning radiometer looks through rectangular apertures in the side and base plate. The low resolution radiometer looks through the round aperture in the base plate almost diametrically opposed to the protruding wide-angle television lens.

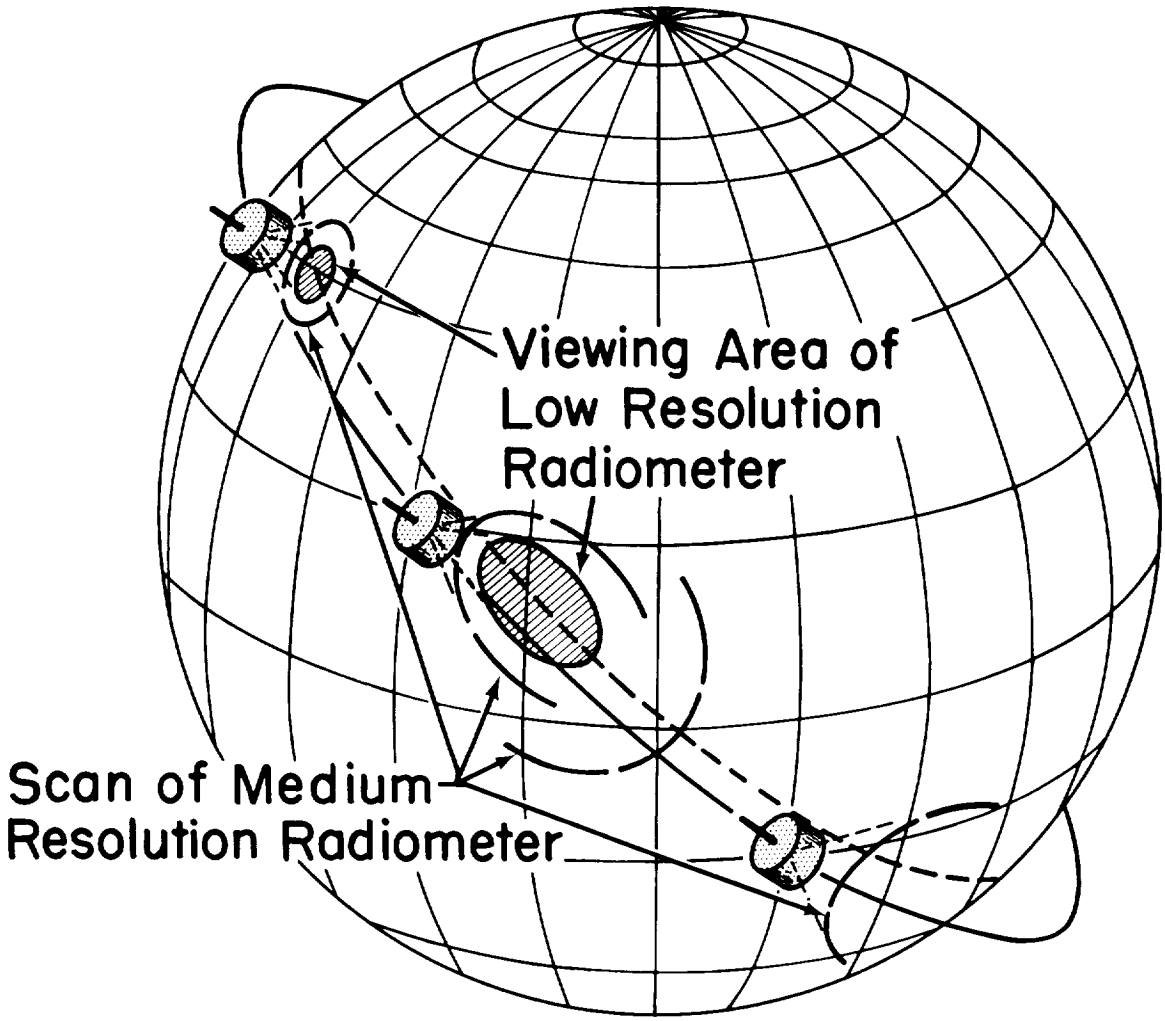

Figure 2—Geometry of the scanning motion of the medium resolution radiometer and of the viewing area of the low resolution radiometer

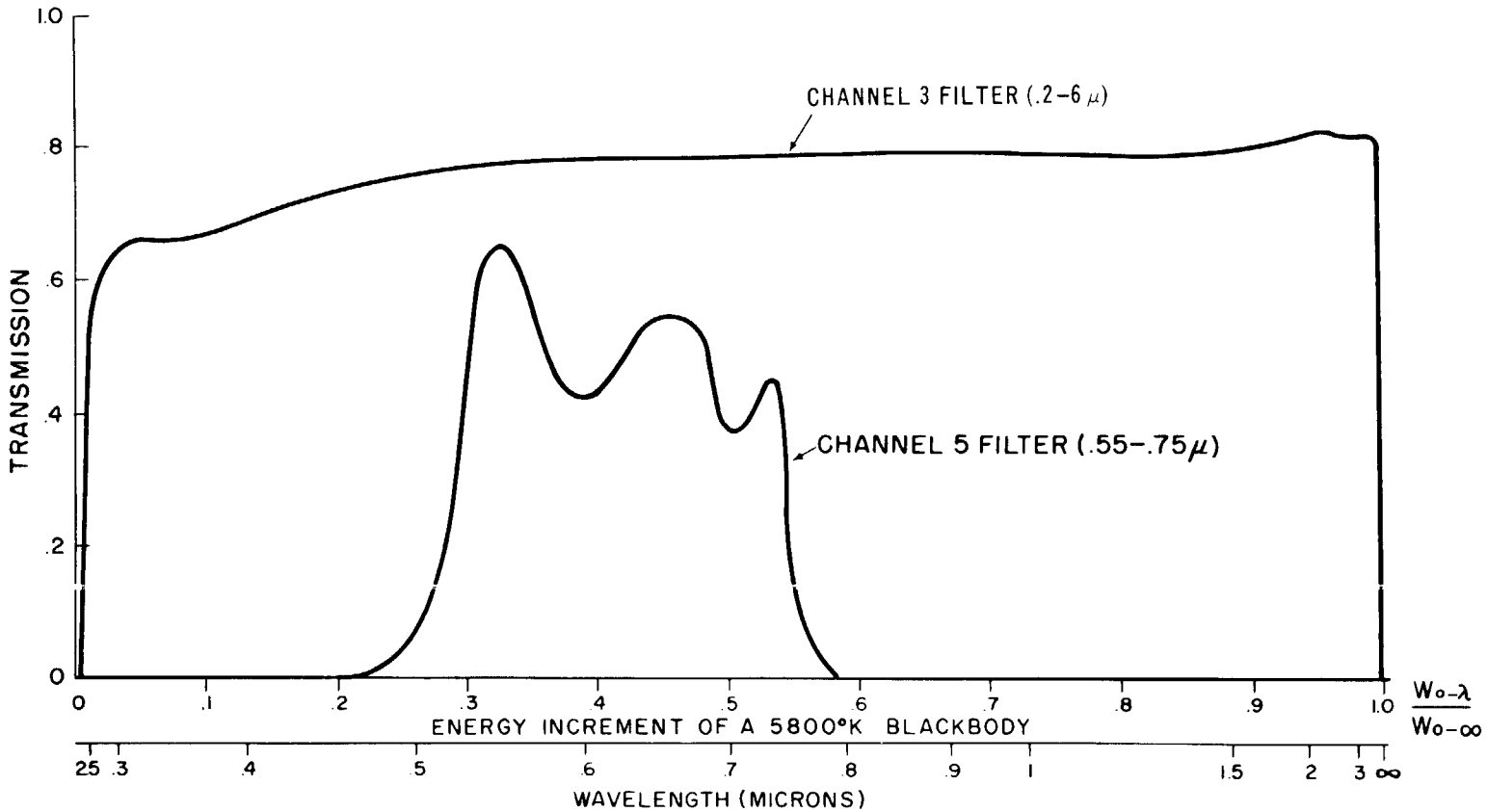

Figure 3—Filter transmission characteristics of channels 3 and 5 of the medium resolution radiometer

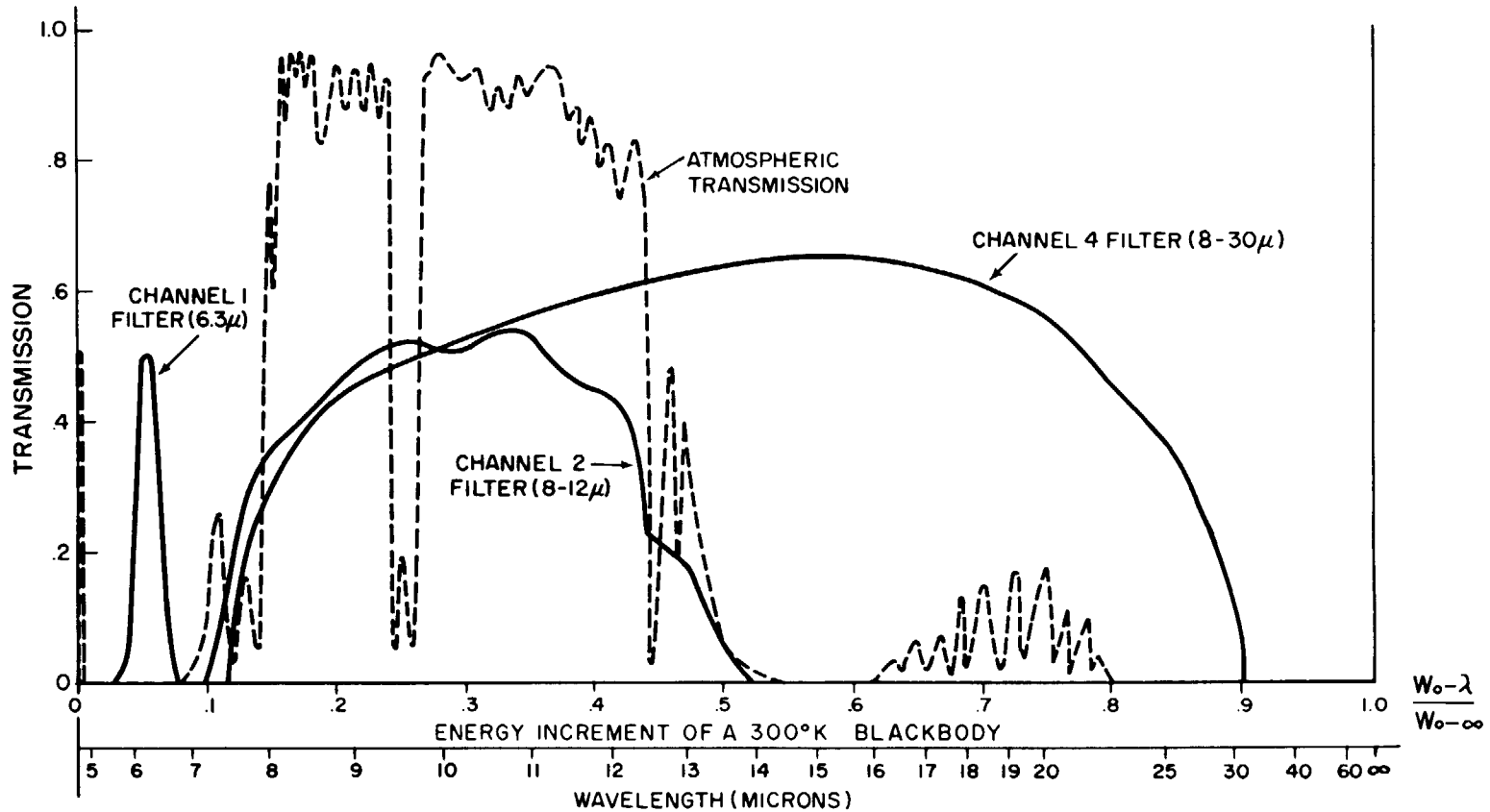

Figure 4—Filter transmission characteristics of channels 1, 2, and 4 of the medium resolution radiometer. The dashed line is the approximate transmission characteristic of one atmosphere.

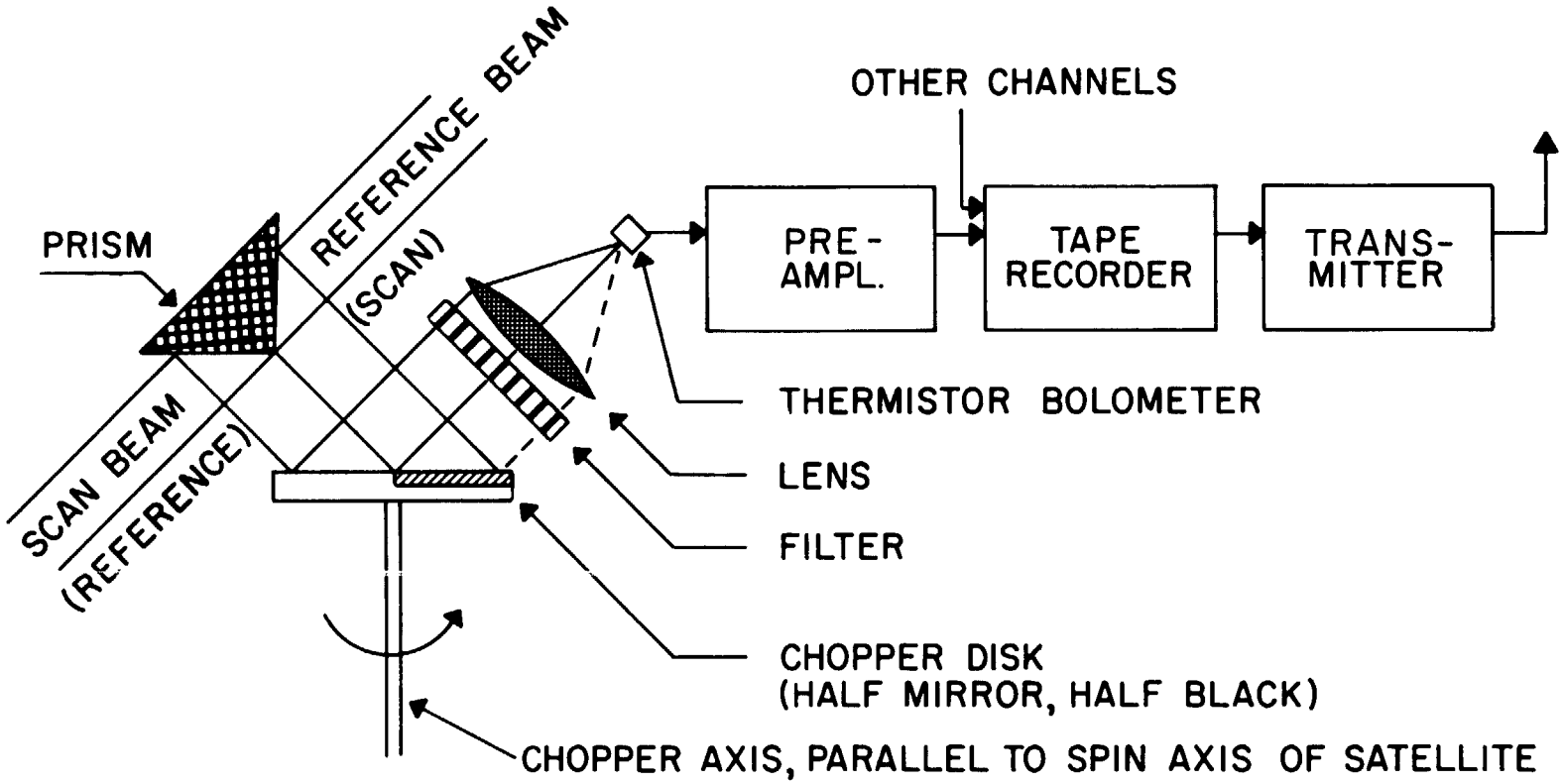

Figure 5—Block diagram of one channel of the medium resolution radiometer

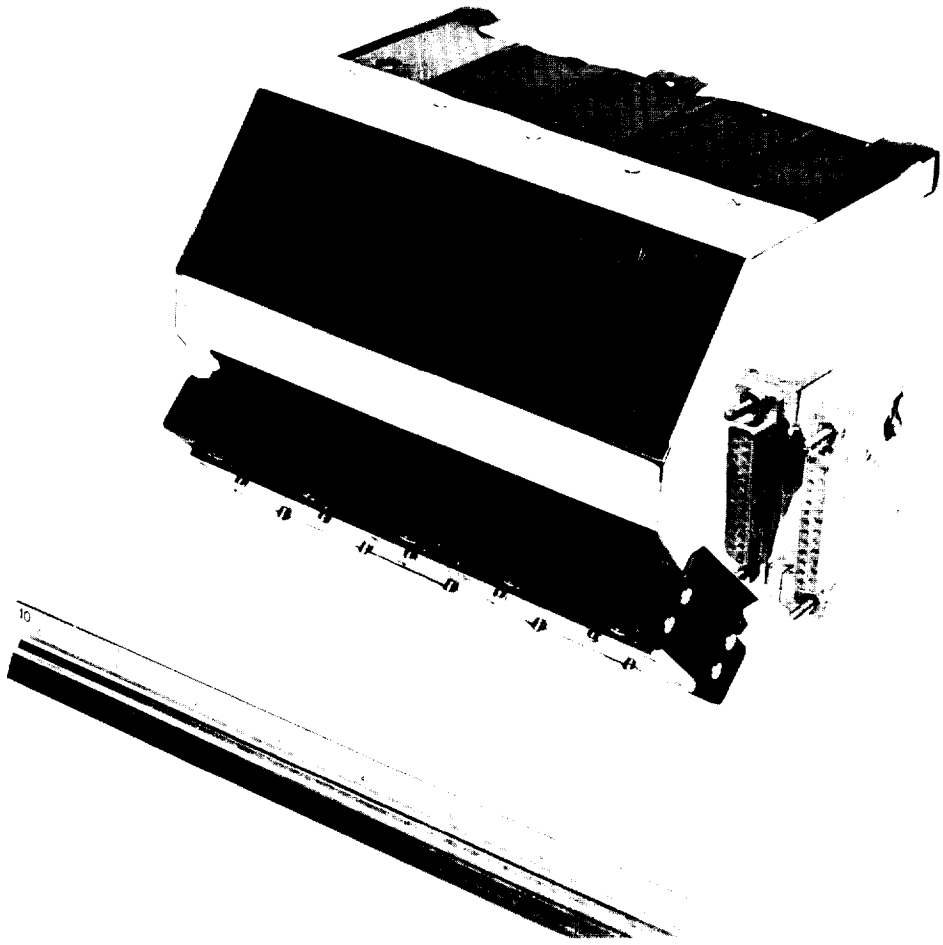

Figure 6—Exterior view of the medium resolution radiometer showing the view apertures in one direction of the five channels. The prismatic cross-section of the reflector is seen on the right of the line of apertures.

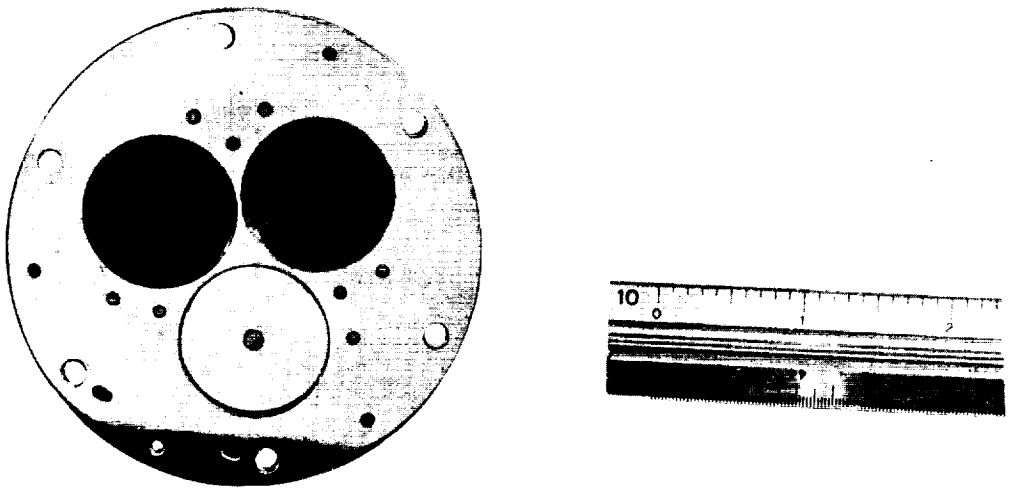

Figure 7—Exterior view of the low resolution radiometer showing the black detector (left) and the white detector (right)

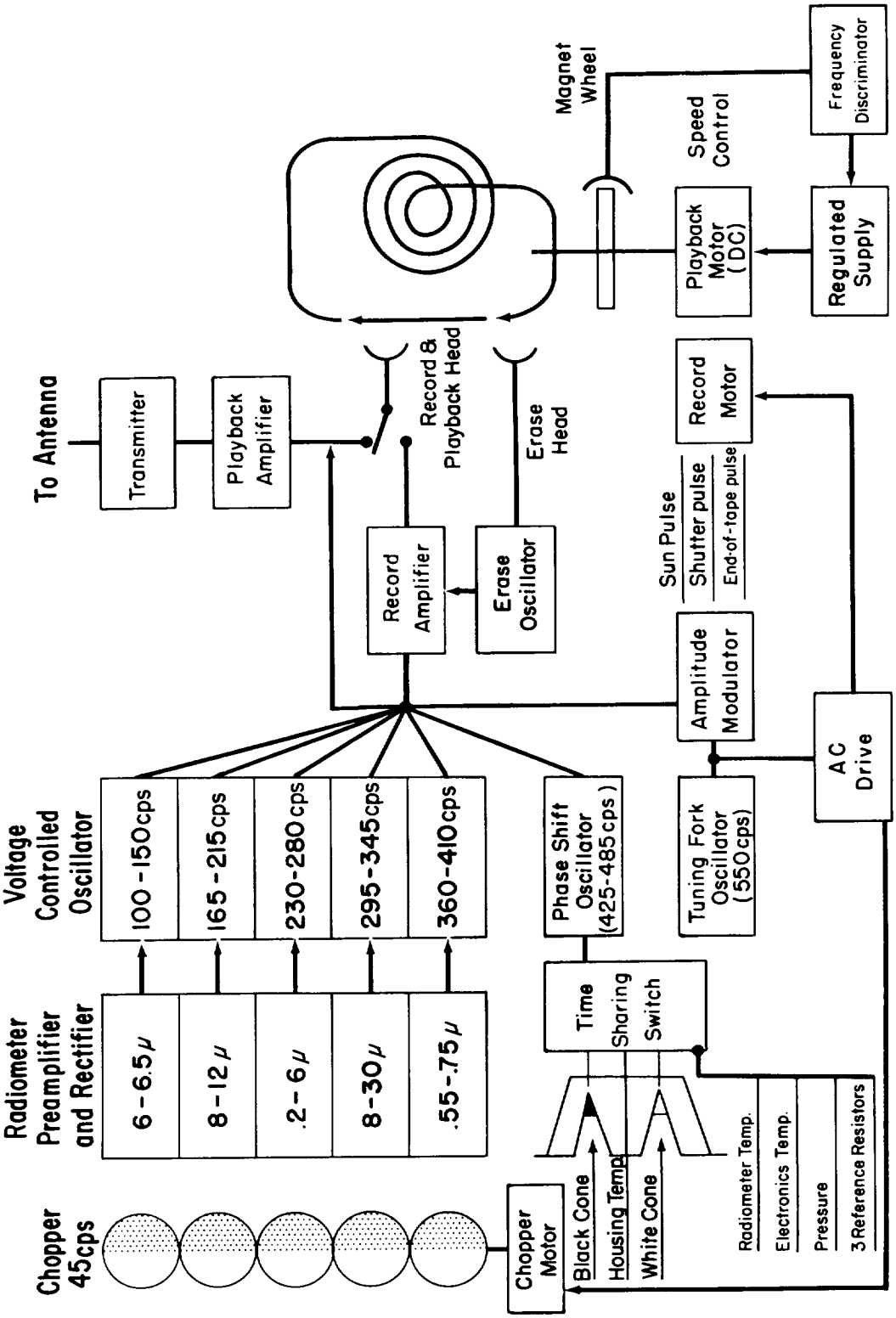

Figure 8—Block diagram of the radiation experiment

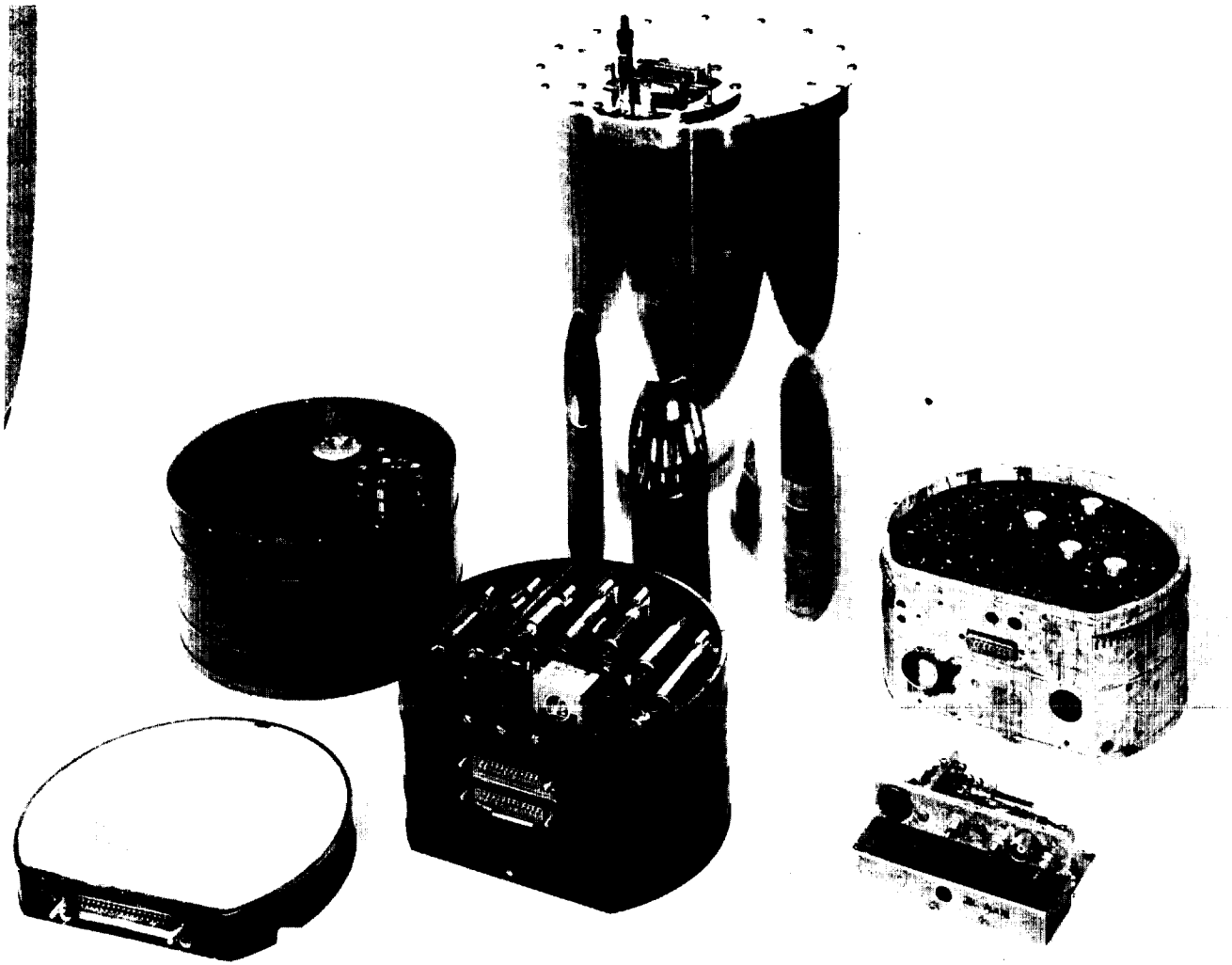

Figure 9—Components of the radiation experiment cannister. From left to right: power supply, tape recorder, main deck electronics, and the 2-watt transmitter which fits into the housing to the right rear which also contains the tape recorder motor electronics. All components fit into the cannister to the center rear.

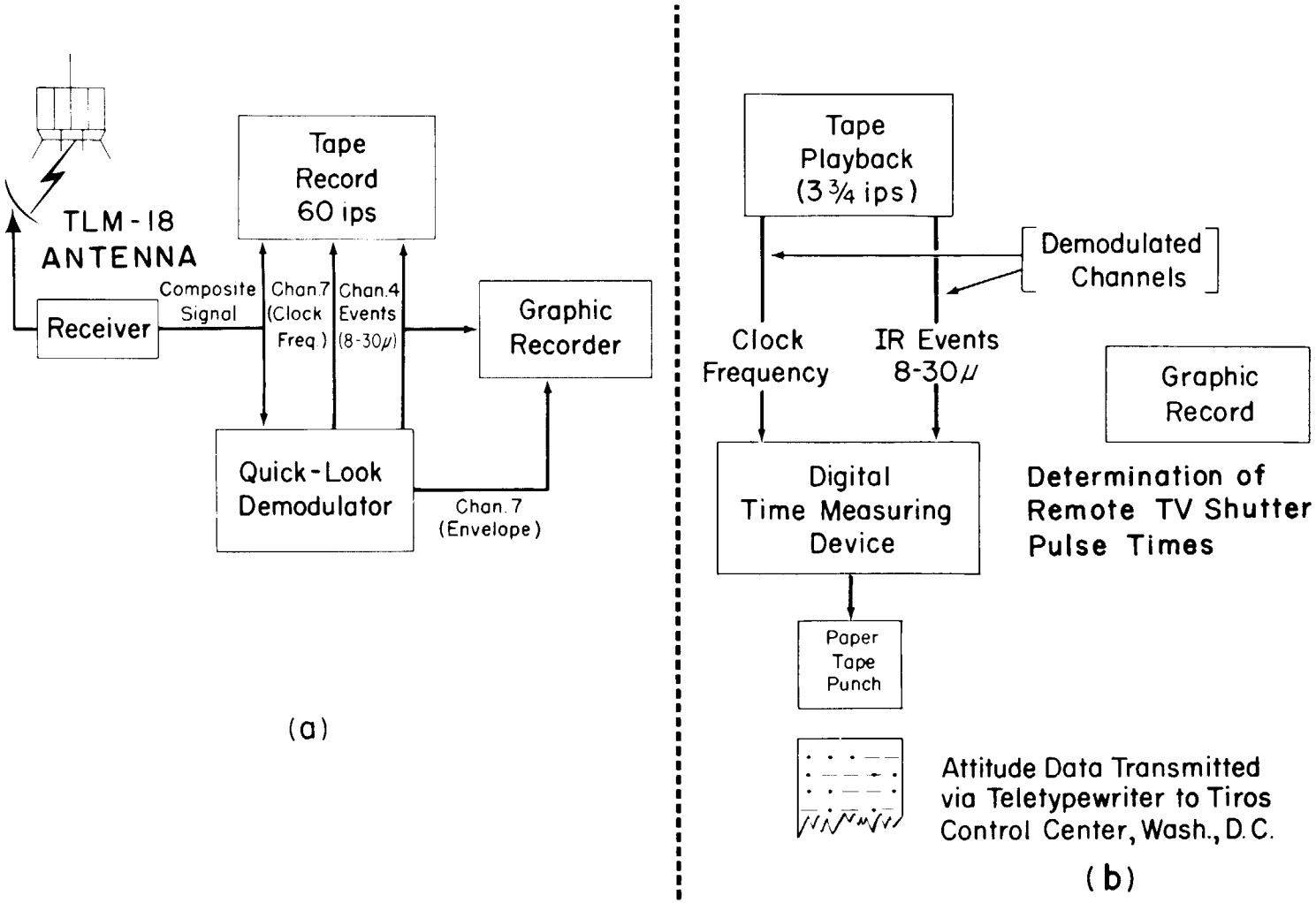

Figure 10—Block diagram of information flow at a data acquisition station including auxiliary uses of the radiation data

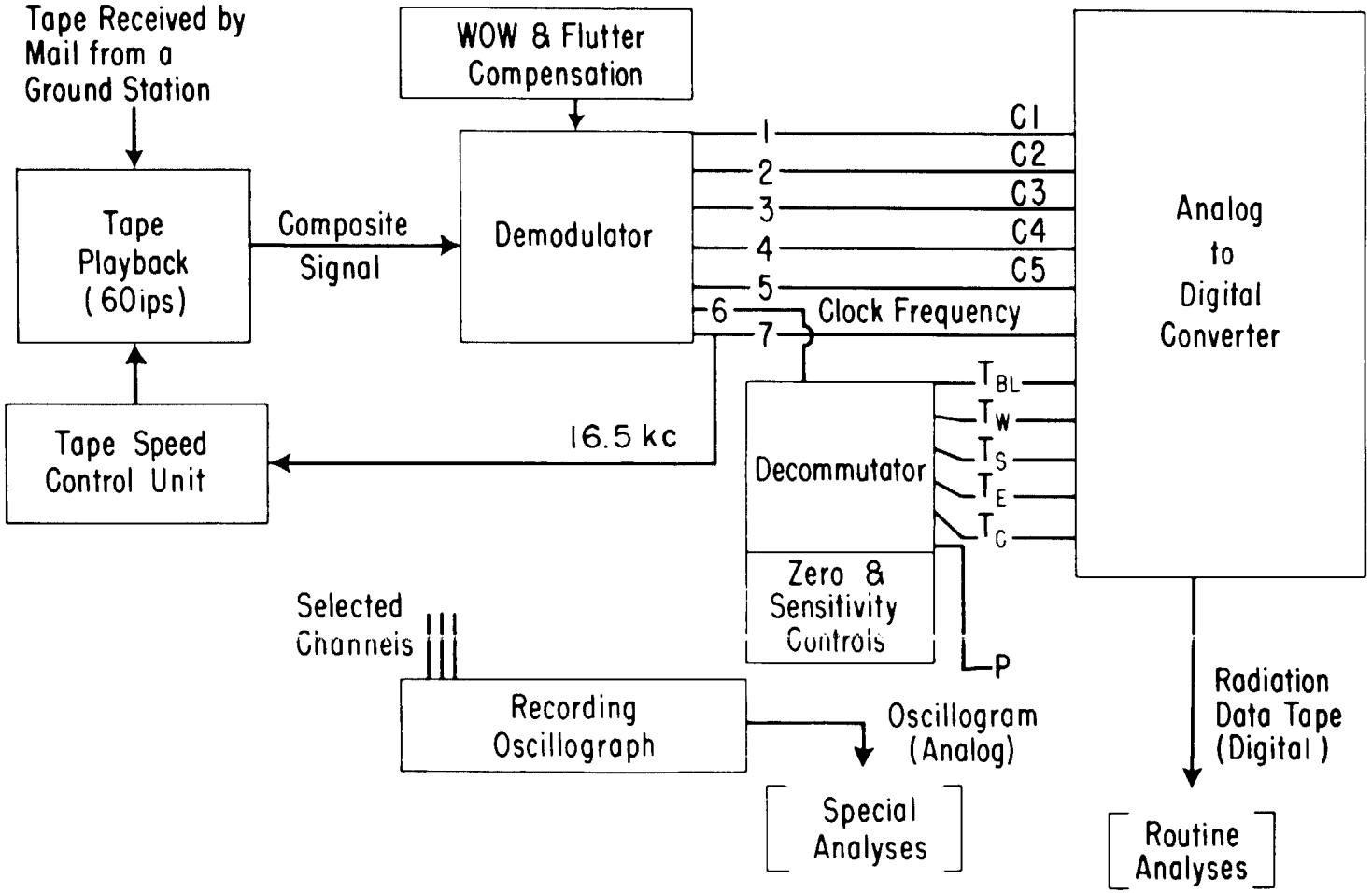

Figure 11—Block diagram of information flow at the data reduction center in producing a digital magnetic tape for computer input. The output of the decommutator consists of temperatures of the black and white cones, three environmental temperatures, and cannister pressure.

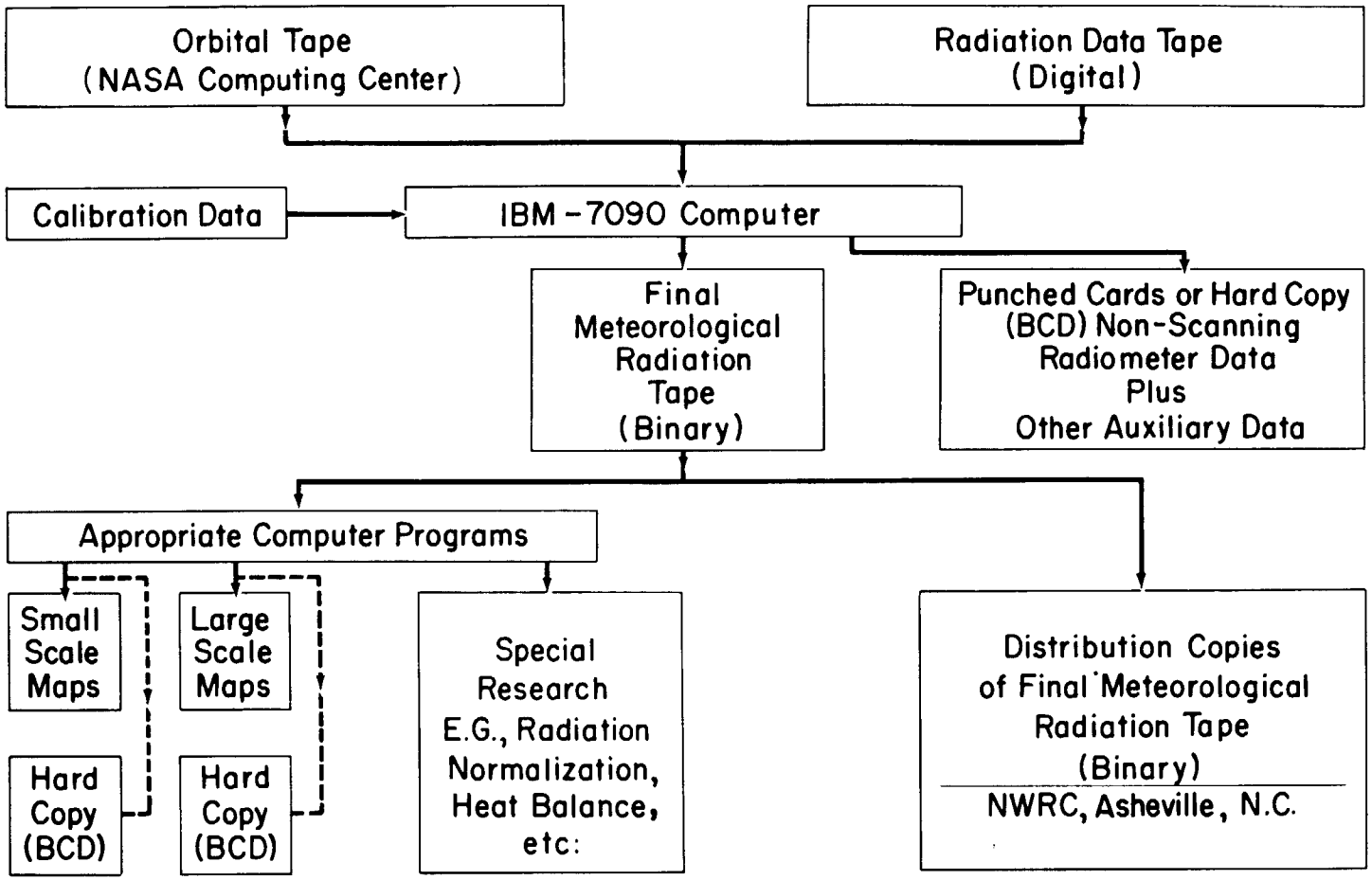

Figure 12—Block diagram of information flow through the IBM 7090 computer at the data reduction center

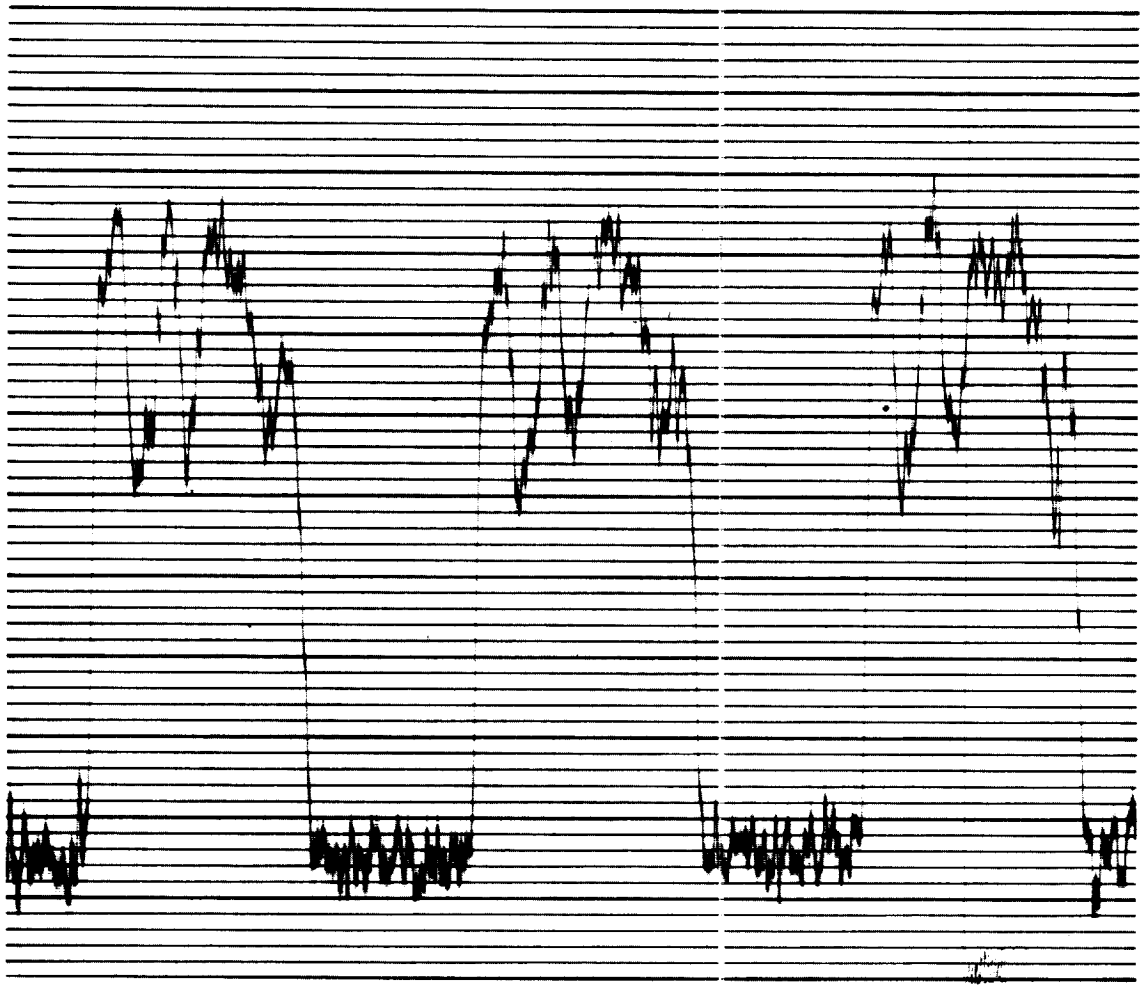

Figure 13—Oscillogram showing three consecutive sky-earth scans of channel 2 of the medium resolution radiometer. The spin period was 7.53 seconds. The amplitude (orcinate) is approximately proportional to the radiant energy received.

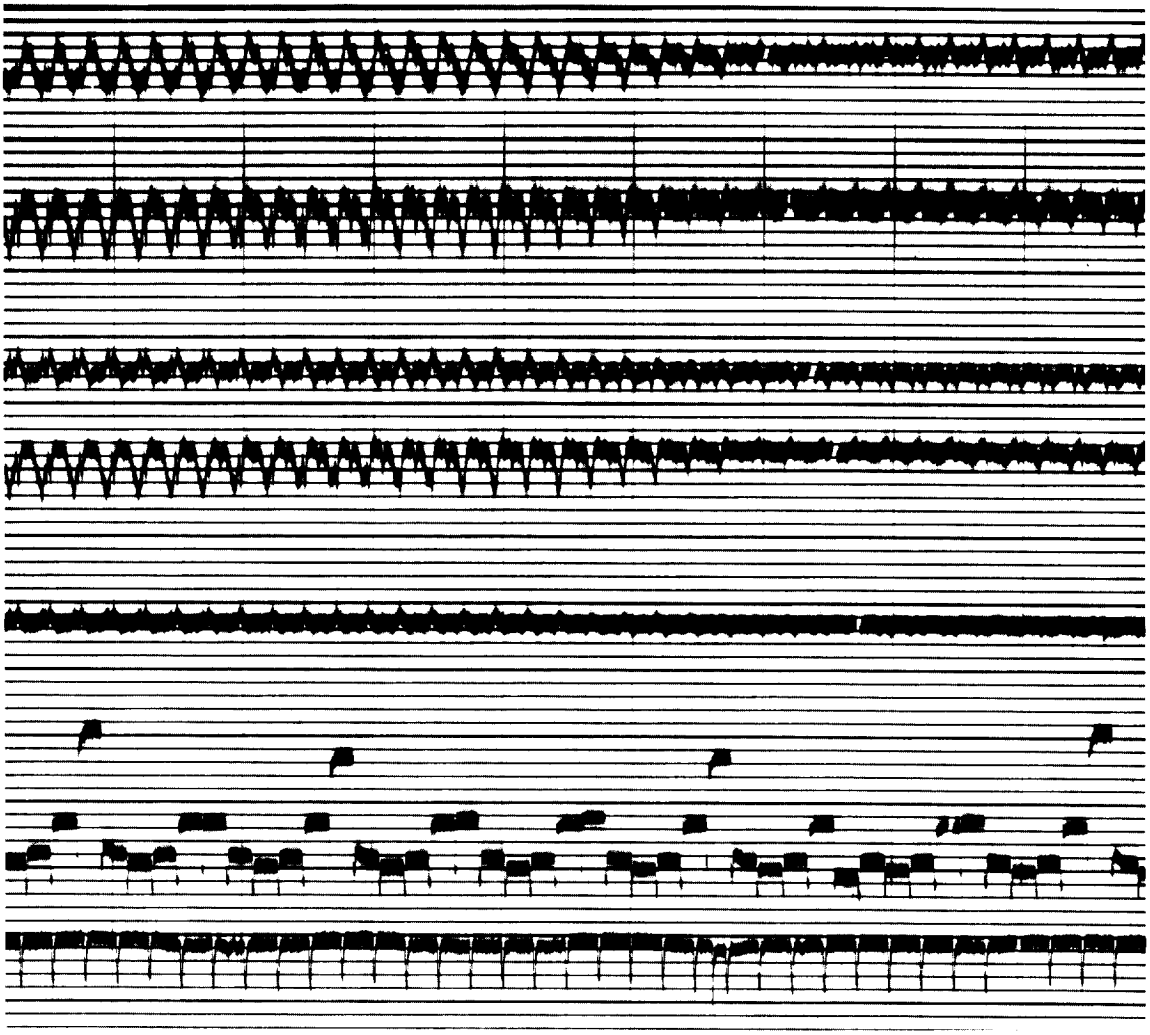

Figure 14—Oscillogram showing all channels of the radiometer experiment. Reading from top to bottom: the five medium resolution channels, the commutated channel 6, and the envelope of the clock frequency showing sun sensor pulses every spin period of 7.53 seconds. The "point of verticality" where one detector sweeps a circle on the earth can be recognized on the right where the horizon is not intercepted at all (see Figure 2).

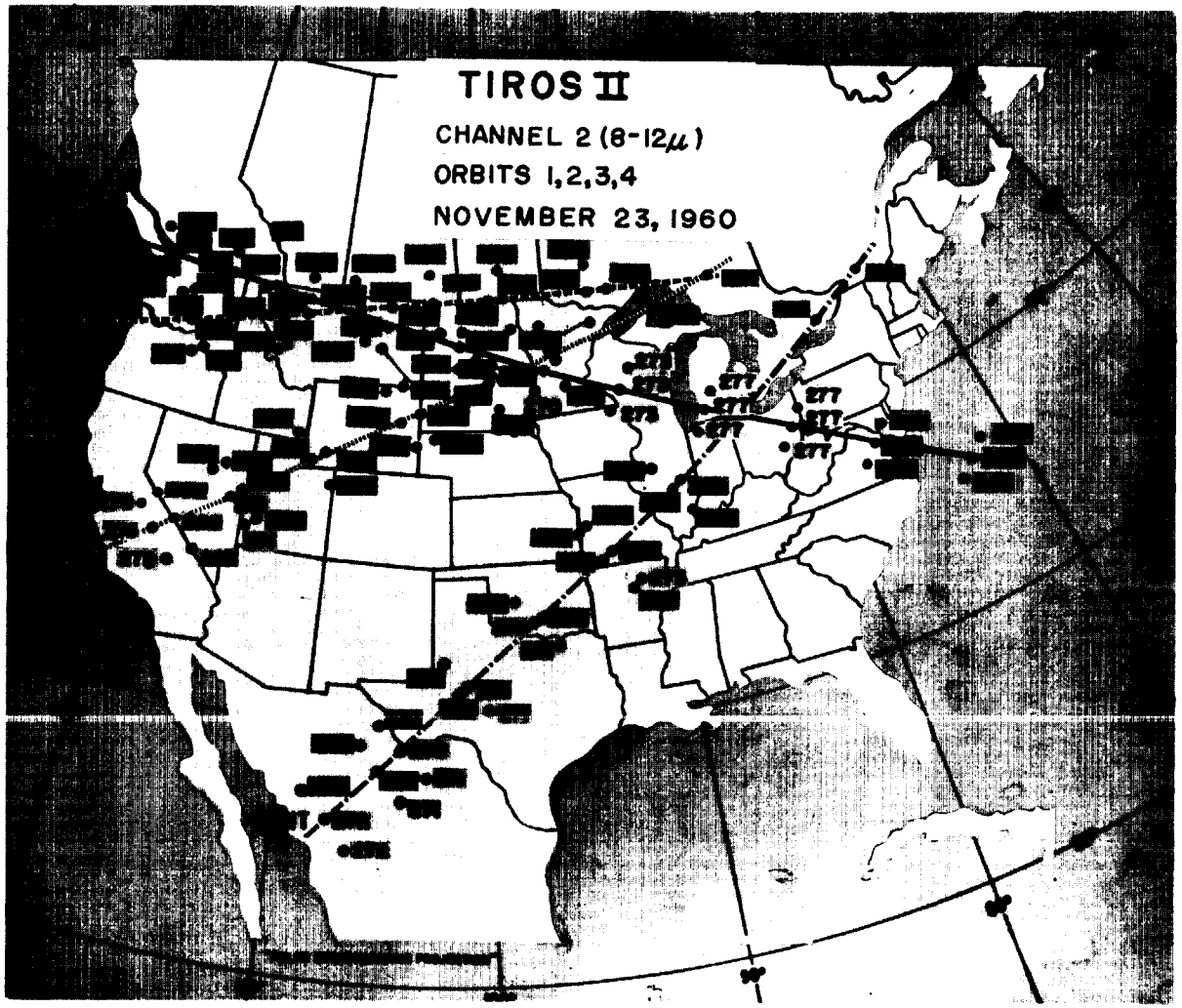

Figure 17—Apparent blackbody temperatures viewed by the 8 to 12 micron channel of the medium resolution radiometer while passing over the United States during the first four orbits after launch, November 23, 1960

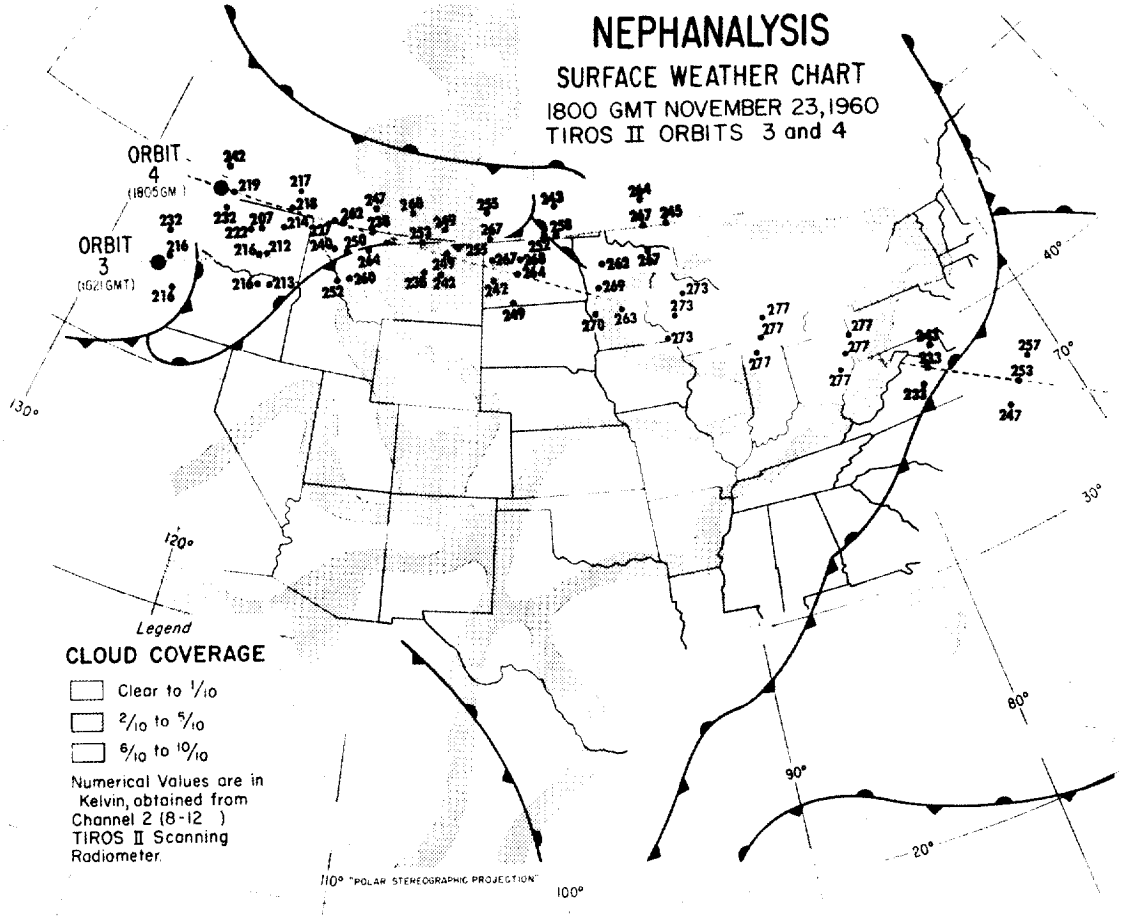

Figure 18—Nephanalysis and frontal position map for 1800 GMT, November 23, 1960. The subsatellite paths, the apparent blackbody temperatures viewed by the 8 to 12 micron channel of the medium resolution radiometer, and the beginning times of the west-to-east passes of orbits 3 and 4 over the United States are shown. Note that maximum temperatures occur over clear areas whereas minimum temperatures occur in the vicinity of largely overcast frontal areas (see Figures 17 and 19).

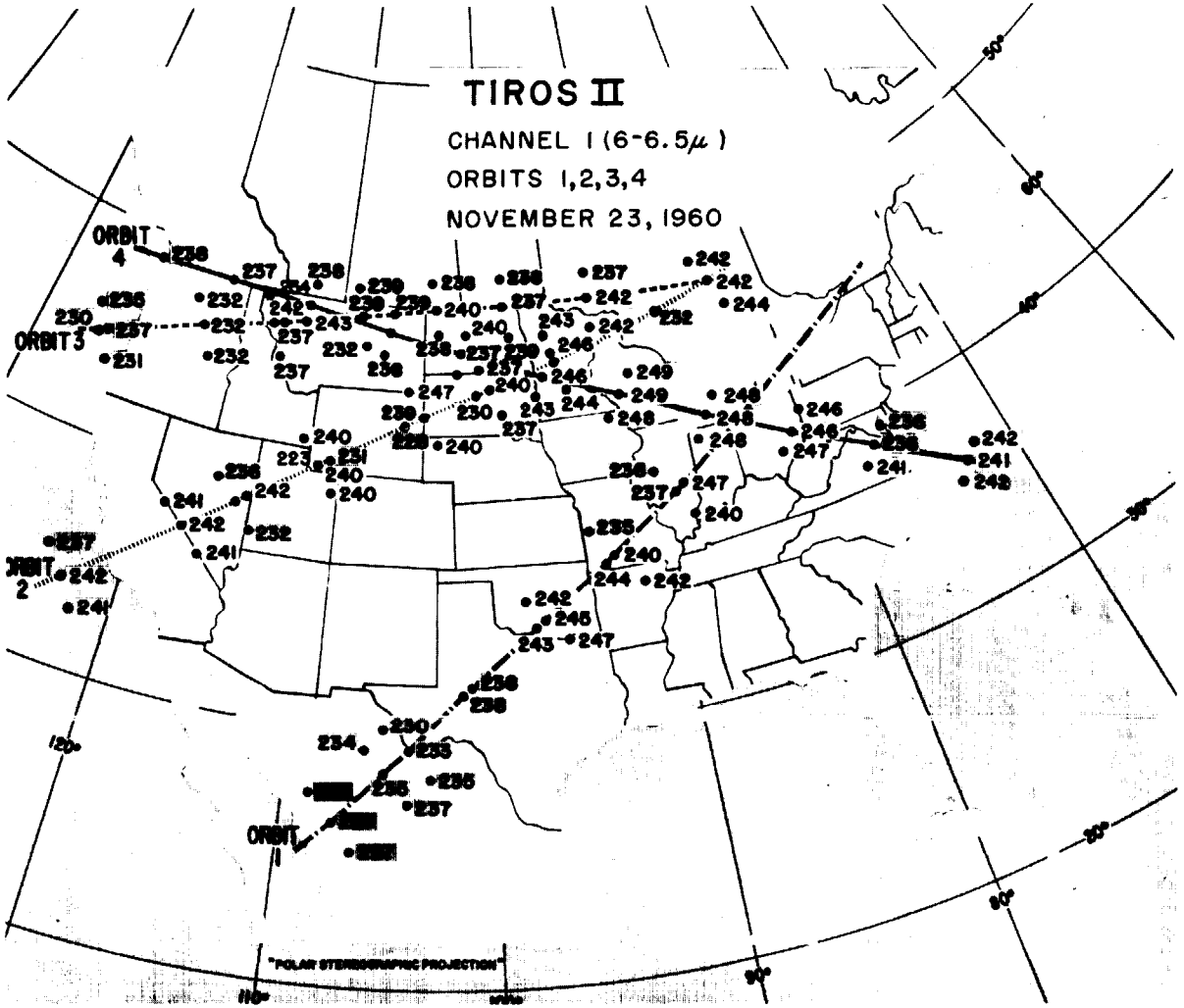

Figure 19—Apparent blackbody temperatures viewed by the 6.0 to 6.5 micron channel of the medium resolution radiometer while passing over the United States during the first four orbits after launch, November 23, 1960

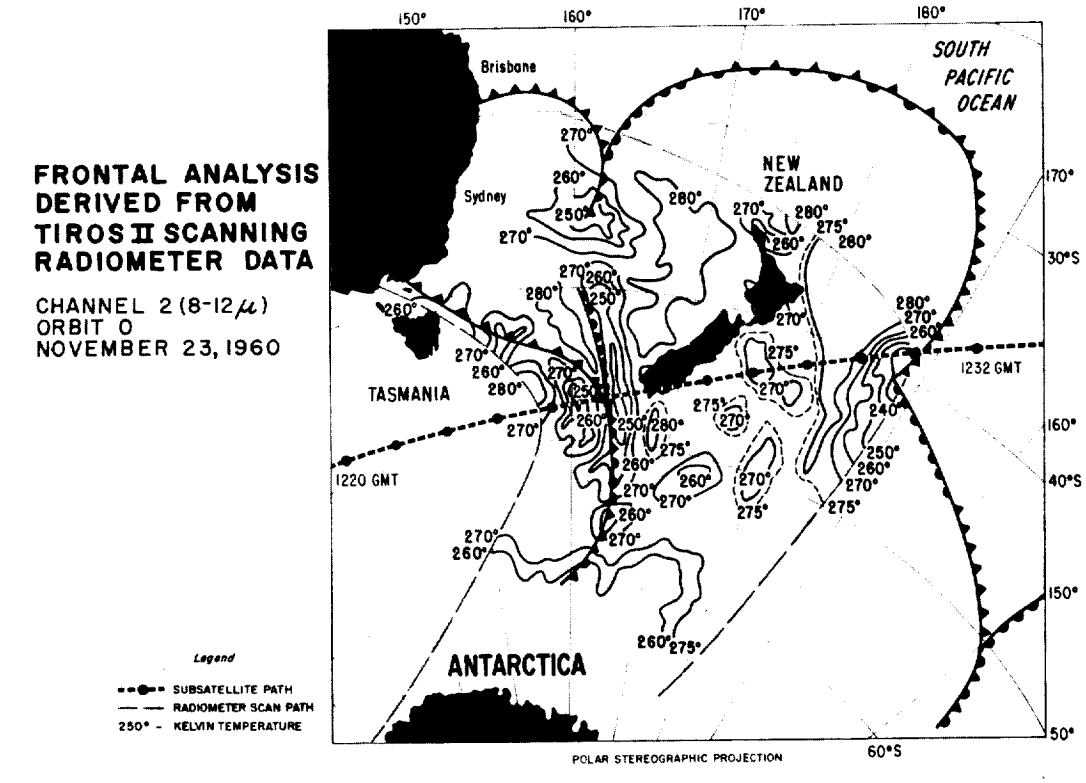

Figure 20—Radiation map constructed from apparent blackbody temperatures viewed by the 8 to 12 micron channel of the medium resolution radiometer while passing over the New Zealand area during orbit "0" just after launch, November 23, 1960. The frontal positions were taken from a standard weather map, based upon limited observations, and modified in accordance with the more voluminous radiation data. Marker dots are placed at 1-minute intervals along the subsatellite path.

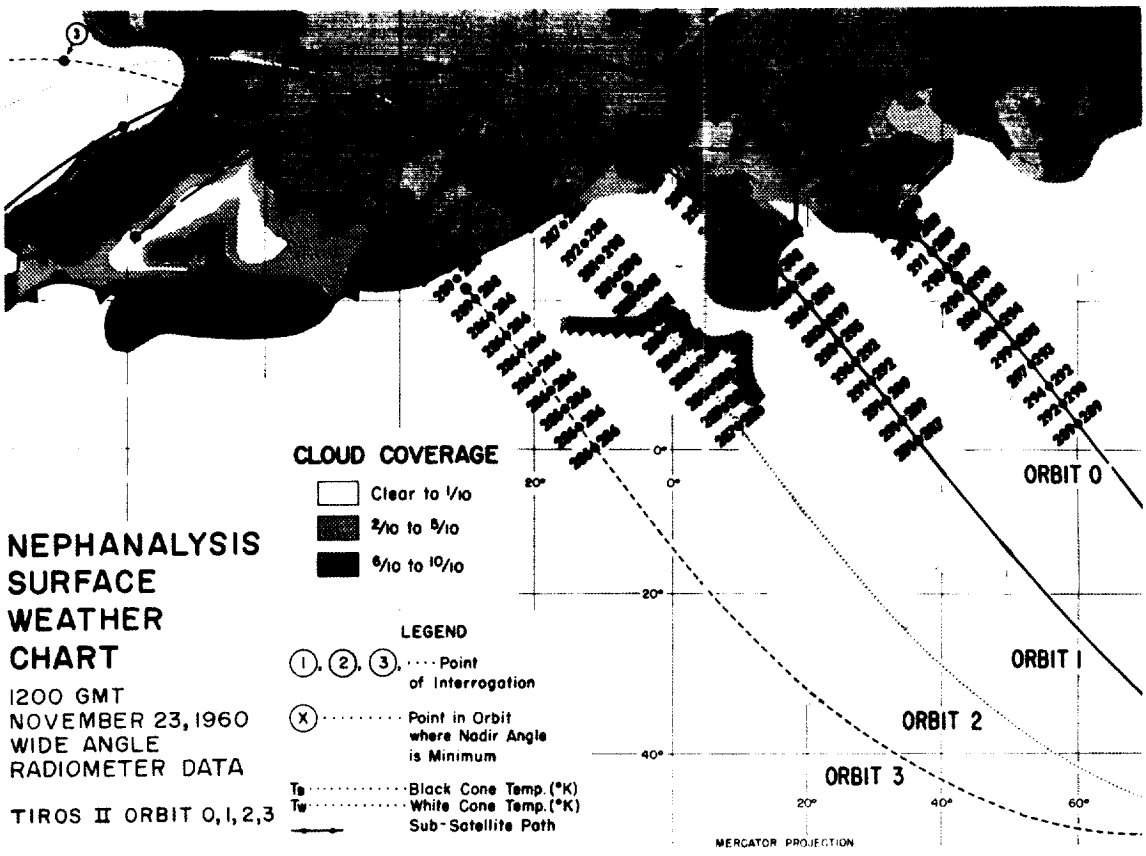

Figure 21—Temperature data from the black and white cones of the low resolution radiometer during orbits 0, 1, 2, and 3 over the Mediterranean, Arabia, Africa, and the Atlantic Ocean, November 23, 1960. The radiometer data are in agreement with the indicated weather data.